

## **Supplementary information**

for

### **Shaping liposomes by cell-free expressed bacterial microtubules**

Johannes Kattan, Anne Doerr, Marileen Dogterom\*, Christophe Danelon\*

Department of Bionanoscience, Kavli Institute of Nanoscience, Delft University of Technology, van der  
Maasweg 9, 2629 HZ, Delft, The Netherlands

\*Correspondence: M.Dogterom@tudelft.nl; C.J.A.Danelon@tudelft.nl

#### **Content**

Supplementary Methods:	S1 – S3
Supplementary Note 1:	S4
Supplementary Note 2:	S5
Supplementary Note 3:	S6
Supplementary Figures	S7 – S14
Supplementary Movies:	S15
Supplementary References:	S16

## SUPPLEMENTARY METHODS

### Sequence of *btubA* (5'→3', complete linear construct)

CAGTCACGACGTTGTAAAACGACGGCCAGTCGCGAAATTAATACGACTCACTATAGGGGAATTGTGAGCGGATAACAA  
TTCCCCTCTAGAAATAATTTTGTTTAACTTTAAGAAGGAGATATACATATGAAAGTTAATAATACAATTGTAGTTAGTAT  
TGGTCAGGCGGGCAACCAAATCGCGGGGAGCTTCTGGAAAACCGTGTGCCTGGAGCACGGTATTGACCCGCTGACCGG  
TCAGACCGCGCCGGGCGTTGCGCCGCGTGGTAACTGGAGCAGCTTCTTTAGCAAGCTGGGCGAGAGCAGCAGCGGTAG  
CTACGTGCCGCGTGCATCATGGTTGATCTGGAACCGAGCGTGTATTGACAACGTTAAAGCGACCAGCGGCAGCCTGTTC  
AACCCGCGAACCTGATTAGCCGTACCGAGGGCGCGGGTGGCAACTTTGCGGTTGGTTACCTGGGTGCGGGTCTGTGAG  
GTGCTGCCGGAAGTTATGAGCCGTCTGGATTATGAAATCGACAAGTGCATAACGTGGGTGGCATCATTGTTCTGCATG  
CGATCGGTGGTGGCACCAGCGCGGTTTTGGCGCGCTGCTGATCGAGAGCCTGAAGGAAAAATACGGCGAGATTCCGG  
TGCTGAGCTGCGCGTCTGCCGAGCCCGCAGGTGAGCAGCGTGGTTACCGAGCCGTATAACACCGTTTTTTCGCTGAA  
CACCTGCGTCGTAGCGGGATGCGTGCCTGATCTTCGATAACGAAGCGCTGTTTGACCTGGCGCACCGTAAATGGAAC  
ATTGAGAGCCCGACCGTGGACGATCTGAACCTGCTGATCACCGAAGCGCTGGCGGGCATTACCGCGAGCATGCGTTTCA  
GCGTTTTTCTGACCGTGAAATCACCTGCGTGAGCTGCTGACCAACCTGGTTCCGCAACCGAGCCTGCACTTCTGAT  
GTGCGGTTTTGCGCCGCTGACCCCGCCGGATCGTAGCAAGTTCGAGGAAGTGGGTATCGAGGAAATGATTAAGCCT  
GTTTCGACAACGGCAGCGTGTTCGCGCGTGCAGCCCGATGGAAGTTCGTTTTCTGAGCACCGCGGTTCTGTATCGTGGC  
ATCATGGAGGATAAACCGCTGGCGGATGCGGCGTGGCGGCGATGCGTGAAAAGCTGCCGCTGACCTACTGGATTCCG  
ACCGCGTTCAAAAATTGGCTATGTTGAGCAGCCGGTATTAGCCACCGTAAAAGCATGGTGTCTGCTGGCGAACAAACCC  
GAAATCGCGCGTGTCTGGATCGTATTTGCCACAACCTTCGACAAGCTGTGGCAACGTAAAGCGTTTTCGAACTGGTATC  
TGAACGAGGGTATGAGCGAGGAACAGATCAACGTGCTGCGTGCAGCGCGCAAGAACTGGTGCAGAGCTATCAAGTTG  
CGGAGGAAAGCGGCGGAAGGCGAAAGTTCAAGACAGCGCGGGTATACCGGTATGCGTGCAGCGGCGGGCGGGTGTG  
AGCGACGATGCGCGTGGTAGCATGAGCCTGCGTGACCTGGTTGATCGTCGCTTAAGCGATCACTAGCATAACCCCTT  
GGGCCTCTAACGGGTCTTGAGGGGTTTTTGGGCGTAATCATGGTCATAGCTGTTTCTGTGTG

### Sequence of *btubB* (5'→3', complete linear construct)

CAGTCACGACGTTGTAAAACGACGGCCAGTCGCGAAATTAATACGACTCACTATAGGGGAATTGTGAGCGGATAACAA  
TTCCCCTCTAGAAATAATTTTGTTTAACTTTAAGAAGGAGATTTGAAAATGAGAGAAATATTAAGTATACATGTAGGTC  
AATGCGGCAACCAGATCGCGGATAGCTTTTGGCGTCTGGCGTGCCTGAACACGGCCTGACCGAGGCGGGCACCTGA  
AGGAAGGTAGCAACGCGGCGGCGAACAGCAACATGGAAGTGTCTCCACAAGGTTCTGACGGTAAATACGTGCCGC  
GTGCGGTGCTGGTTGATCTGGAGCCGGGCGTTATCGCGGTATTGAAGGTGGCGACATGAGCCAGCTGTTTGTGAAAG  
CAGCATCGTGCCTAAAATCCCGGTGCGGCGAACAACTGGGCGCGTGGTTATAACGTGGAGGGCGAAAAAGTTATCGA  
CCAGATTATGAACGTGATCGATAGCGCGGTTGAGAAGACCAAAGGTCTGCAAGGCTTCTGATGACCCATAGCATCGG  
TGGCGGTAGCGGCAGCGGTCTGGGCAGCCTGATTCTGGAACGTCTGCGTCAGGCGTACCCGAAGAAACGTATCTTACC  
TTTAGCGTGGTTCCGAGCCGCTGATTAGCGACAGCGCGGTGGAGCCGTATAACGCGATCCTGACCTGCAACGTATTC  
TGGACAACGCGGATGGTGCAGTTCTGCTGGACAACGAAGCGCTGTTCCGTATCGCGAAGGCGAAACTGAACCGTAGCC  
CGAACTACATGGATCTGAACAACATCATTGCGCTGATTGTGAGCAGCGTTACCGCGAGCCTGCGTTTTCCGGGCAAGCT  
GAACACCGATCTGAGCGAGTTCGTGACCAACCTGGTTCCGTTCCCGGGCAACCACTTTCTGACCGCGAGCTTCGCGCCG  
ATGCGTGGTGCAGGTCAGGAAGGTCAAGTGCCTACCAACTTTCCGACCTGGCGCGTGAACCTTTGCGCAGGACAAC  
TTCACCGCGGCGATCGATTGGCAGCAAGGTGTTTATCTGGCGGCGAGCGCGCTGTTCCGTGGCGATGTGAAGGCGAAA  
GACGTTGATGAAAACATGGCGACCATTCGTAAGAGCCTGAACTACGCGAGCTATATGCCGCGAGCGGCGGTCTGAAA  
CTGGGCTATGCGGAAACCGCGCCGGAAGGTTTTGCGAGCAGCGCCTGGCGCTGGTGAACCACACCGGTATCGCGGCG

GTTTTGAGCGTCTGATCGCGCAATTCGACATTATGTTTGATAACCACGCGTACACCCACTGGTATGAAAACGCGGGTG  
TTAGCCGTGACATGATGGCGAAAGCGCGTAACCAGATTGCGACCCTGGCGCAGAGCTATCGTGATGCGAGCTAAGCAA  
TAACTAGCATAACCCCTTGGGGCCTCTAAACGGGTCTTGAGGGGTTTTTTGGGCGTAATCATGGTCATAGCTGTTTCCTG  
TGTG

### **Sequence of *btubC* (5'→3', from T7 promoter to T7 terminator)**

TAATACGACTCACTATAGGGGAATTGTGAGCGGATAACAATTCCCCTCTAGAAATAATTTTGTTTAACTTTAAGAAGGA  
GATATACATATGGGCAGCAGCCATCATCATCATCACAGCAGCGGCCTGGTGCCGCGCGGCAGCATGGACTCCCCTC  
TCGATCGTCAGCTCGCTGCCGCCTCTCGCAGTGTGGAAGAGGCGCGGAGAATGGCTTATCACGACGATTCTGAAGATCGG  
GTATCTGGTGGAGCAGATCAGCGTGCTGGCAGATCTGCGGCAGAAAGAGGGAGACTTCCGCAAGGCCGAGTCGCTGTA  
TCGTGAGGCGCTATTCAGCGCTCAGGAGCAGCGTAAGCCGGACCCGGAGTTGCTGACGGGCATCCATTCCTTGCTGGCG  
CATCTGTATGATCGCTGGGGCCGGATGGATCTCGCCTCGCAGTTTTATGAGAAAGCCCTGAAGATCGCCGAGCGAGGGCG  
GCATCGCCAGAGTGATAAGGTGGCGATCATCAAAAACAATCTGGCGATGATCTTCAAGCAGTCCGTGACTACACCC  
GTGCGGAGCAGCACTACCAAGAGGCGCTGAAATCTTCCGCAAAACGGATGGTGAATACAGCGCTCGGGTGGCTAGCG  
TTTTTAACAATCTCGGGGTGCTATATTACAGCAACCTGGAGGTGAGCAGGCCGAGGAGATGCATGAGCATGCGTTGAC  
GATTCGGCAGAGCCTTTCGAATGATCAGGCGGACTCGGGGGATCTCTCACAGACCTACATCAATCTCGGCGCTGTTTAT  
AAAGCGGCGGGAGATTTTCAGAAAGCTGAGGCCTGTGTGGATCGTGCTAAGAAGCTGCGGGCCAGCATGAATGGCTAC  
CACCCGAGCCGCGCCGTGCGGCGTCTTTGCTTGTGATAAATCCCTGTGACAAAGCCCGAAAGGAAGCTGAGTTGGCT  
GCTGCCACCGCTGAGCAATAACTAGCATAACCCCTTGGGGCCTCTAAACGGGTCTTGAGGGGTTTTTTG

### **Vesicle flotation assay**

Liposomes were prepared according to the protocol used to generate SUVs, as described in the main text Methods, with slight modifications. The lipid film (1000 µg) was resuspended with 100 µL of a solution consisting of a 1:3 dilution of PURE $_{flex}$ 2.0 with MilliQ water (10 mg mL<sup>-1</sup> final concentration) and vortexed for 5 min. A 20-µL PURE $_{flex}$ 2.0 reaction mix containing the appropriate DNA construct was incubated for 3 h at 37 °C. The DNA construct *btubC* was designed as described in the main text Methods for the *btubA* and *btubB* templates. Twelve microliters of a liposome solution were added and the sample was incubated for 20 min at 30 °C. Next, 80 µL of a 1:1 dilution of PURE $_{flex}$ 2.0 Solution-I (buffer Solution) with MilliQ water was added and the sample was spun down at 8,000 g for 2 min. After centrifugation, the lighter vesicles formed a pellet at the top of the solution. Eighty microliters of solution underneath the pellet were harvested. The pellet was subjected to a second centrifugation, another 15 µL of the bottom solution was removed and the pellet was resuspended by pipetting up and down. Of this liposome fraction, 10 µL was collected for analysis. The 80-µL solution of the bottom fraction from the first centrifugation was spun down and a 10-µL sample taken from the middle of the tube was harvested for analysis. Equal amounts of liposome and bottom fractions were loaded on a 12% SDS-PAGE gel.

## **SUPPLEMENTARY NOTE 1: Interaction of BtubA/B/C with the vesicle membrane**

We examined the activity of cell-free expressed BtubA/B/C by conducting liposome floatation experiments (Fig. S4A). BtubC was produced and co-translationally labelled with GreenLys before incubation with lipid vesicles. After centrifugation, samples were collected from the liposome (upper) and bulk (lower) fractions, loaded on gel, and the BtubC protein content was analysed by fluorescence imaging. A clear enrichment of BtubC in the liposome fraction was observed, indicating binding to the lipid membrane (Fig. S4C). The ability of BtubC to interact with bMTs [1,2] was assessed by supplementing the solution with purified BtubA/B. In this assay, BtubC was unmodified (expression without GreenLys) and 1.2  $\mu\text{M}$  of purified BtubA/B, including 100 nM of tubulin labelled with the dye Atto488, were employed. The protein mix and lipid vesicles were incubated to enable polymerization of bMTs and membrane binding. Sample was centrifuged and the partitioning of BtubA/B between the liposome and bulk fractions was analysed by gel imaging. BtubA/B was noticeably enriched in the liposome fraction (Fig. S4B). This result demonstrates that cell-free expressed BtubC is able to recruit BtubA/B to lipid membranes. In the absence of BtubC, purified BtubA/B was found in both the liposome and bulk fractions. It has been reported that purified BtubC interacts with polymerized BtubA/B but not with tubulin monomers or dimers [1]. Therefore, BtubC-conditional recruitment of BtubA/B to lipid vesicles would suggest formation of bMTs. Cell-free expressed, GreenLys-labelled BtubA/B incubated with lipid vesicles partitioned in both the liposome and bulk fractions (Fig. S4C). When all three proteins BtubA/B/C were co-expressed, enrichment of BtubA/B in the liposome fraction was visible (Fig. S4C), suggesting polymerization of cell-free expressed tubulin. Together, these results demonstrate that in vitro synthesized BtubC can bind to lipid membranes, where it recruits bMTs composed of cell-free expressed BtubA/B. The fact that BtubA/B was found also in the liposome fraction in the absence of BtubC suggests weak binding with membranes, this interaction being promoted by BtubC. Moreover, BtubC has been reported to stabilize BtubA/B filaments [2], which may favour the recruitment of long bMTs to lipid membranes.

We do not know the mechanism by which bMTs interact with an SLB. Commonly found mechanisms in membrane-protein interactions are (i) specific lipid-protein binding (e.g. annexins, C2 domains), (ii) the presence of an amphipathic helix (e.g. MinD, FtsA) and (iii) electrostatic interactions between negatively charged lipids and a protein domain with positive surface charges (e.g. cationic toxins, cytochrome c). Structural investigations of bMT did not reveal features that would clearly point to a membrane-binding domain [2]. Therefore, we believe that weak electrostatic interactions may cause bMTs to associate to lipid bilayers in our conditions (presence of the negatively charged lipids phosphatidylglycerol and cardiolipin).

## **SUPPLEMENTARY NOTE 2: Relationship between the concentration of expressed BtubA/B and the liposome morphology**

The type and the degree of the morphological changes of liposomes are the result of competitive forces between the membrane tension, the pushing forces of the growing microtubules and the rigidity of the bundle. In particular, the concentration of encapsulated monomers and the polymerization state of filaments are important control parameters of the pushing force exerted by the bMT to the membrane. Using purified BtubA/B, we found that encapsulated 6.6  $\mu\text{M}$  of monomers assemble into long bMT bundles that drastically change liposome morphology (long protrusions, star-shapes, see Fig. 5). We also know that 1  $\mu\text{M}$  of purified BtubA/B form short bMTs that are very likely not able to span the entire lumen of the liposomes (Fig. S5), while a concentration of 2.5  $\mu\text{M}$  yields bMT bundles with lengths  $> 20 \mu\text{m}$  (Fig. 2A), which is larger than the typical diameter of liposomes ( $< 15 \mu\text{m}$ , see Fig. 4 and Fig. S6). Therefore, the monomer concentration threshold to induce liposome deformation is  $> 1 \mu\text{M}$ . For concentrations comprised between 1  $\mu\text{M}$  and  $\sim 6 \mu\text{M}$ , liposomes are expected to undergo shape transformation that resemble those observed in Fig. 4 and Fig. S6. Typical morphologies include lemon-shape with straight bundles spanning the lumen, elongated liposomes with a complex network of bMTs and asymmetrically deformed liposomes exhibiting a short protrusion. For liposomes that elongate in a quasi-symmetrical manner, an aspect ratio of 2 or lower can be estimated. Importantly, these considerations do not take into account the polymerization state of BtubA/B, which might differ between purified and expressed tubulin proteins in PURE system (see below).

After 3 hours of co-expression in bulk reactions, the cumulative concentration of BtubA and BtubB is  $\sim 8 \mu\text{M}$  (Fig. S3). We know from previous measurements in the laboratory that the typical gene expression kinetics can be represented by a sigmoidal function with a time-to-plateau of about 3 hours and an apparent maximum translation rate in the order of  $\sim 40 \text{ nM/min}$  [3]. Assuming similar properties with the *btubA/B* genes, estimated values of tubulin concentration would be  $\sim 10 \mu\text{M}$  after 300 minutes (typical imaging time) and  $\sim 2 \mu\text{M}$  after 60 minutes, time at which the first bMTs become clearly visible (Fig. S6). At both concentrations, the extent of morphology changes is less than expected on the basis of the behavior with purified proteins, suggesting that the polymerization rate is reduced with expressed BtubA/B. This latter effect might be explained if not all expressed tubulin are functional, for instance due to misfolding or aggregation. Alternatively, the pool of GTP might decline, or the balance of  $\text{Mg}^{2+}$  might change in the course of gene expression, which would impair tubulin polymerization and bMT stability.

In summary, we recommend to use purified BtubA/B at concentrations  $> 6 \mu\text{M}$  to drastically deform liposomes. For producing elongated liposomes with a ratio of the long- and short-axis  $\leq 2$ , either purified tubulin proteins with concentrations  $> 1 \mu\text{M}$  but  $< 6 \mu\text{M}$  or in-vesicle expressed proteins can be used. In the latter condition,  $> 2$  hours of expression is necessary to obtain a significant number of bMT-deforming liposomes.

### **SUPPLEMENTARY NOTE 3: Comparison between eukaryotic and bacterial MTs**

To compare the behavior of eukaryotic and bacterial microtubules, purified  $\alpha$ - and  $\beta$ -tubulin proteins (purchased from tebu-bio B.V., Netherlands) were encapsulated in PURE system-containing liposomes (without DNA) following the protocol established for bMTs. This is important because the inner/outer osmolarity, the ionic and lipid compositions may influence the polymerization rate and the membrane tension, and consequently the liposome morphology and the organization of the entrapped microtubules. Fig. S8 shows that eukaryotic microtubules can arrange into bundles with three characteristic morphologies, as already reported in [4-7]: (i) A single straight bundle that spans the lumen of the liposome and forms two membrane protrusions opposite to each other, a phenotype known as phi ( $\phi$ ) shape. (ii) A ring at the membrane that tends to deform the liposome into an oblate spheroid. (iii) single bended or buckled microtubule bundles that can deform the membrane. These properties are markedly different than with bMTs (Fig. 4, Fig. S6), which can be attributed to the higher rigidity of eukaryotic microtubules.

## SUPPLEMENTARY FIGURES

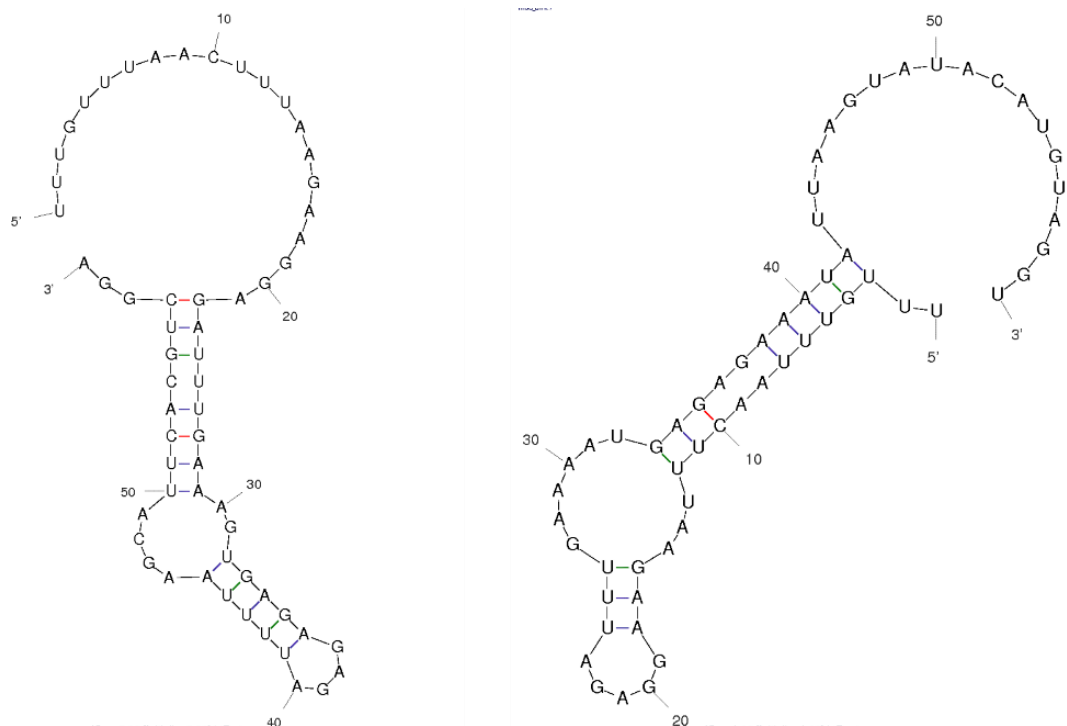


**Figure S1:** Possible RNA structures of the 30 bp sequence before and after the start codon (including start codon, 60 bp total). The structures with the lowest  $\Delta G$  values were calculated with mfold [8] for the sequences comprising the RBS in combination with either the wildtype sequence (left image,  $\Delta G = -5.8 \text{ kcal mol}^{-1}$ ) or the optimized sequence (right image,  $\Delta G = -1.0 \text{ kcal mol}^{-1}$ ).

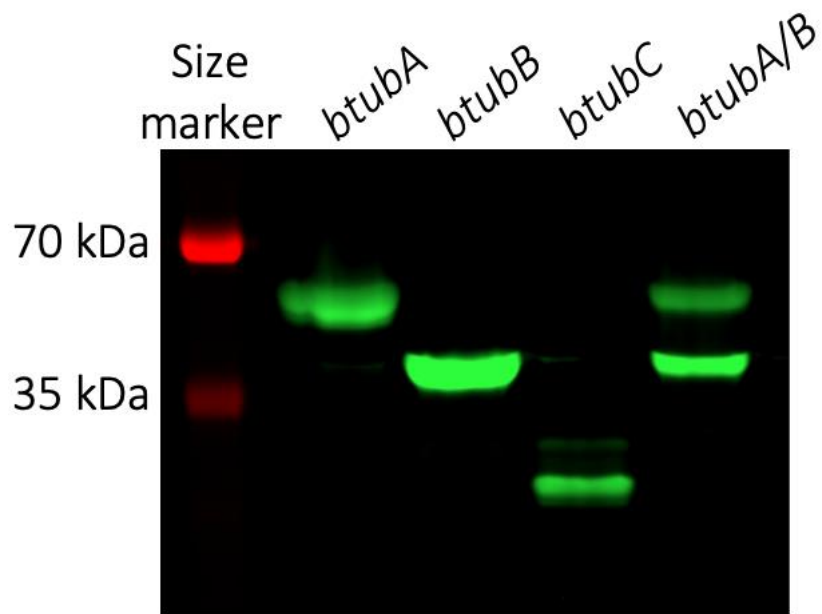


**Figure S2:** Fluorescence image of the SDS-PAGE gel shown in main text Fig. 1. Here, the lane with sample of expressed *btubC* gene is uncropped.



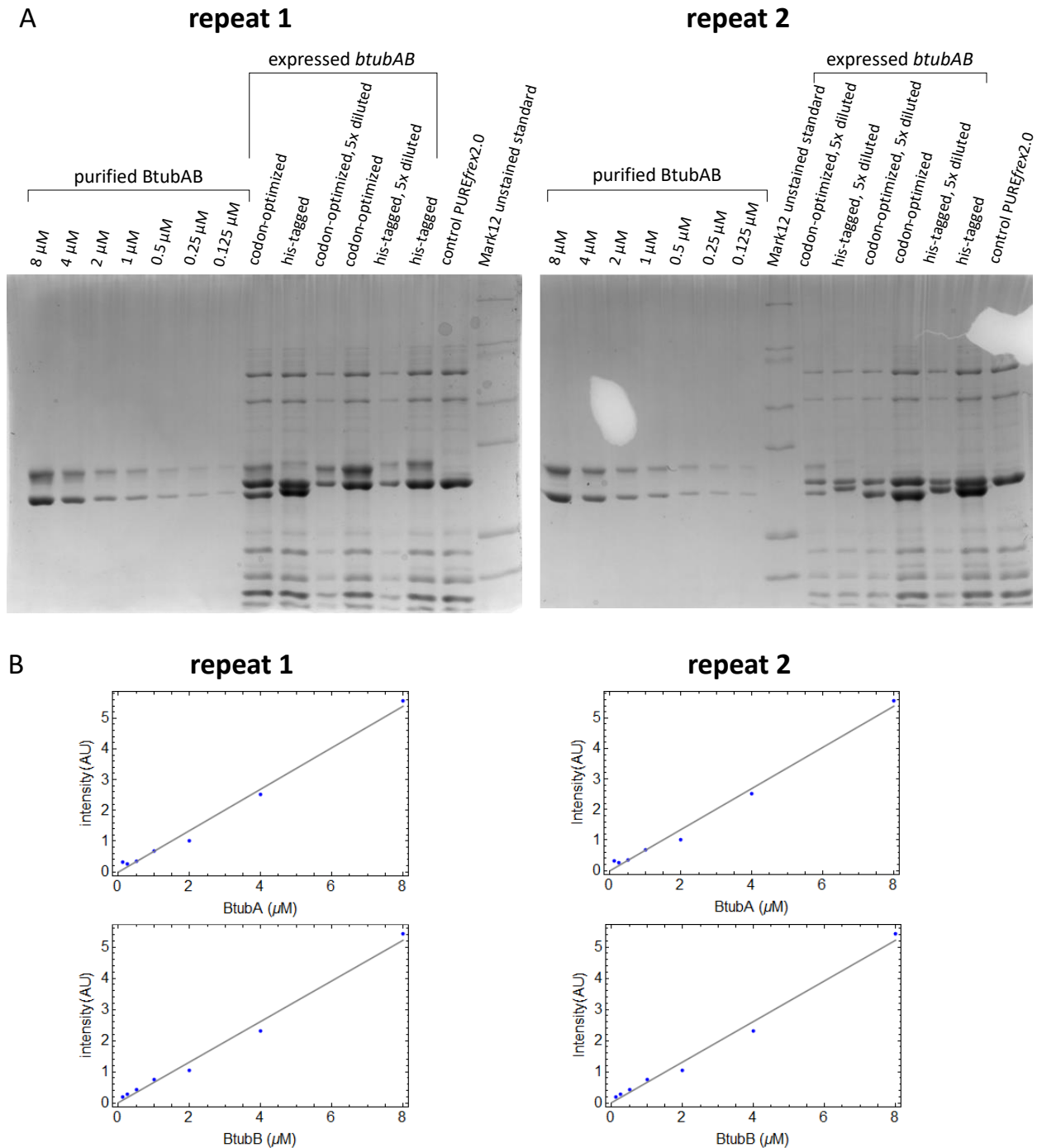


**Figure S3:** Estimation of the concentrations of expressed BtubA/B. (A) Samples of expressed and purified BtubA/B proteins were analysed by SDS-PAGE. Purified proteins were loaded at different concentrations ranging from 0.125 to 8  $\mu\text{M}$ . DNA constructs of the wild-type (his-tagged) or optimized *btubA/B* gene sequences were used as templates in PURE $_{refx2.0}$  bulk reactions. A control sample with no DNA was also prepared. Data from two independent repeats are shown. (B) Calibration curves for BtubA and BtubB were plotted by measuring the band intensity on gel for each concentration of the purified proteins. Data from the two independent experiments in (A) are shown. The measured band intensity for the 5  $\times$  diluted and undiluted PURE $_{refx2.0}$  samples was used to extract the concentration of expressed BtubA/B.

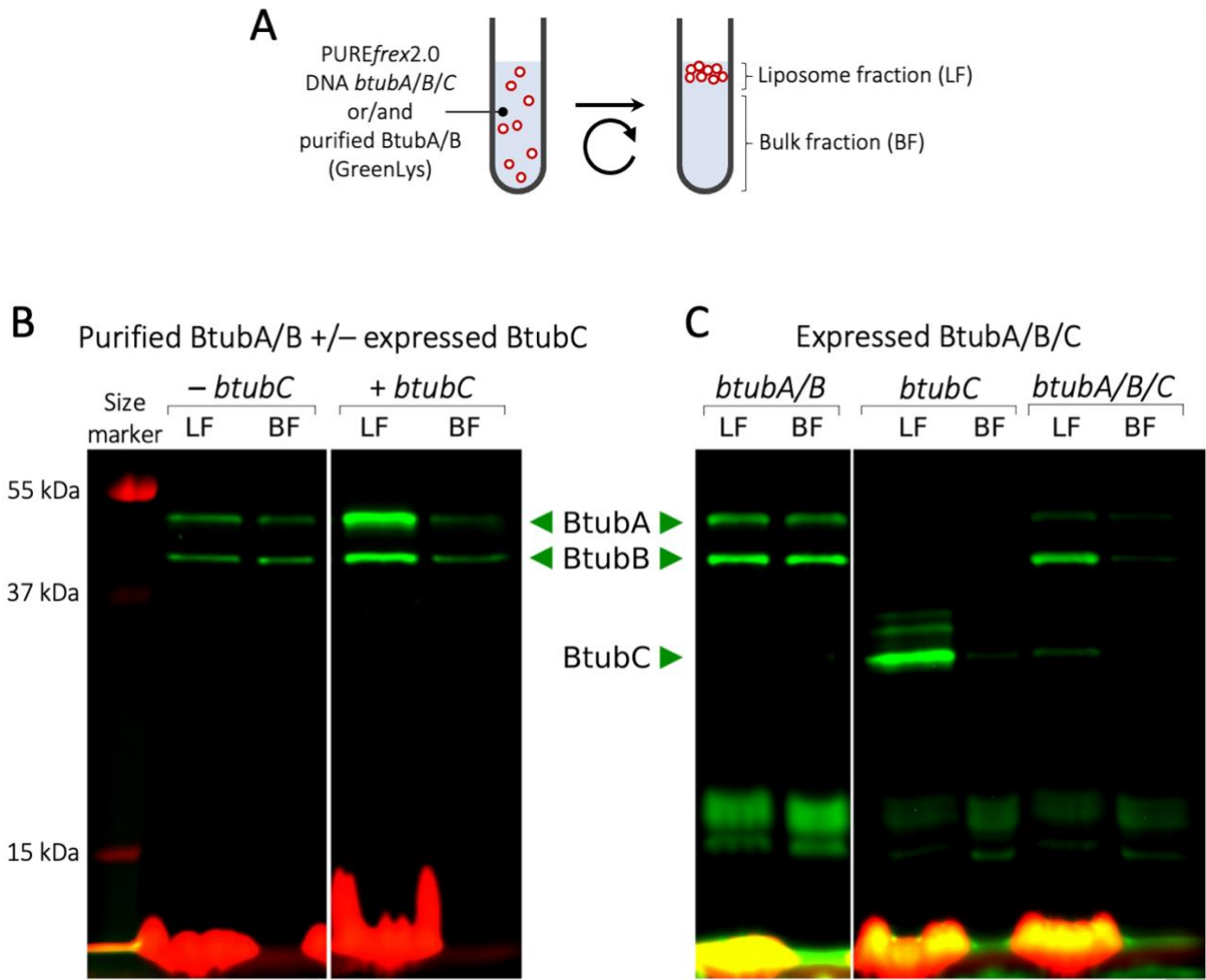


**Figure S4:** Activity of cell-free expressed BtubA/B/C characterized using a vesicle floatation assay. (A) Schematic of the vesicle floatation assay. Liposomes (coloured in red) were incubated with purified or/and pre-expressed BtubA/B/C in PUREfrex2.0. When appropriate, the GreenLys reagent was included in the CFPS reaction. Alternatively, a fraction of purified, labelled Alexa488-BtubA/B was used for tubulin visualization by gel imaging. After centrifugation, a floating pellet of vesicles formed. Proteins interacting with the vesicles were enriched in the liposome fraction (LF) compared to the bulk fraction (BF). (B, C) SDS-PAGE analysis of BtubA/B/C partitioning between LF and BF. (B) A small amount of Alexa488-BtubA/B was used to visualize BtubAB filaments and study the ability of expressed BtubC to recruit them to the vesicle membrane. (C) BtubA/B/C were expressed with GreenLys in different combinations as indicated with the gene names. The red signal at the bottom of the lanes results from the DHPE-TexasRed lipids of the vesicles and is therefore stronger in the liposome fractions.

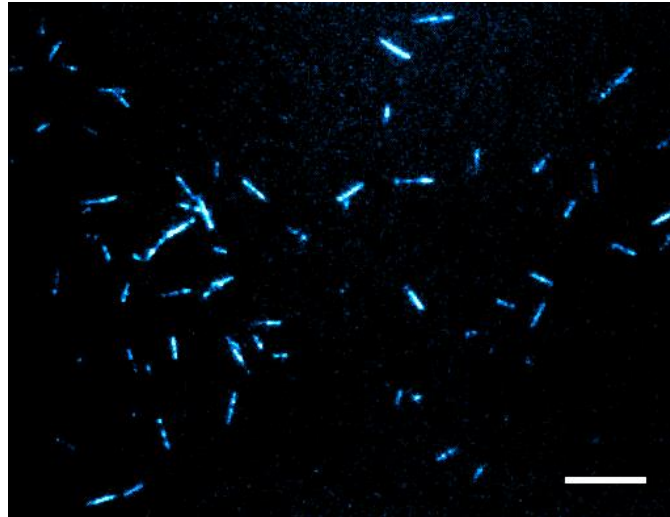


**Figure S5:** Fluorescence image of bMTs formed by 1  $\mu\text{M}$  of purified BtubA/B on an SLB. Scale bar: 10  $\mu\text{m}$ .

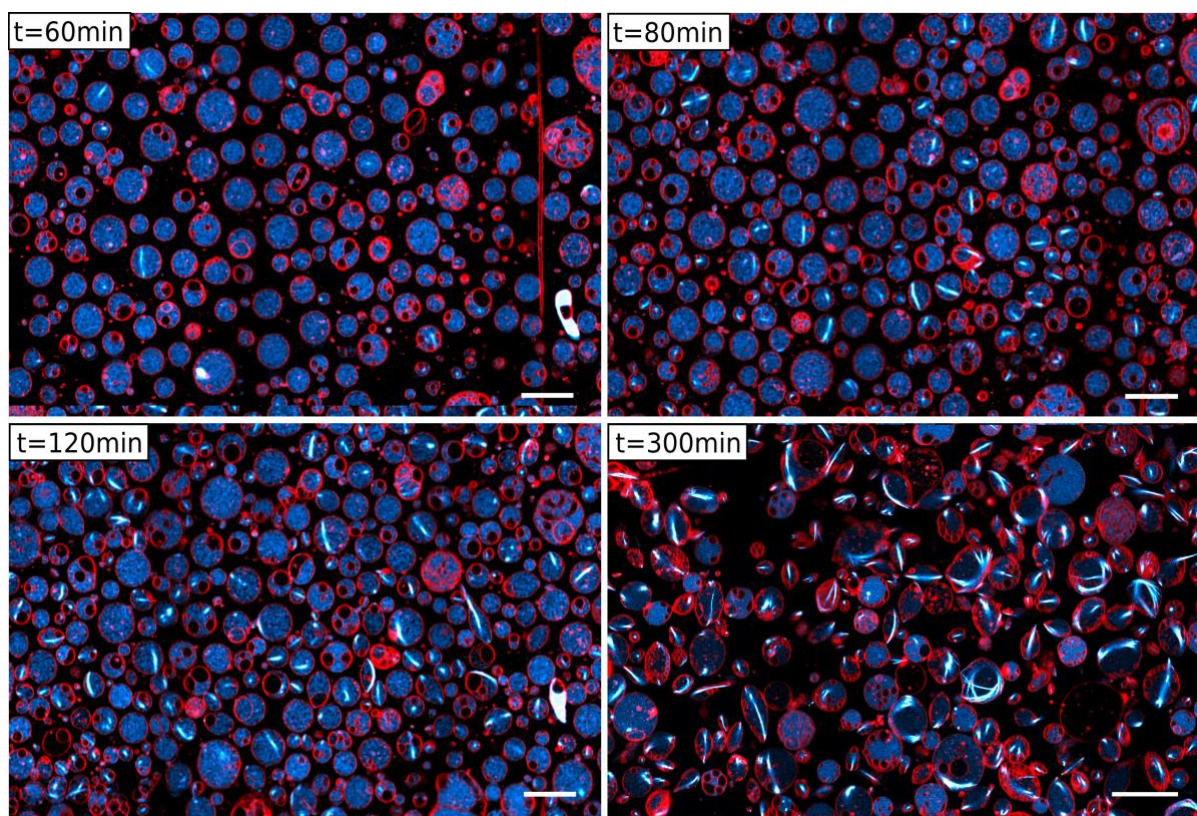


**Figure S6:** Time lapsed images of bacterial tubulin expression inside liposomes. Incubation was conducted at 37 °C. The time of incubation at which the images were acquired is appended. Scale bars: 20 μm.

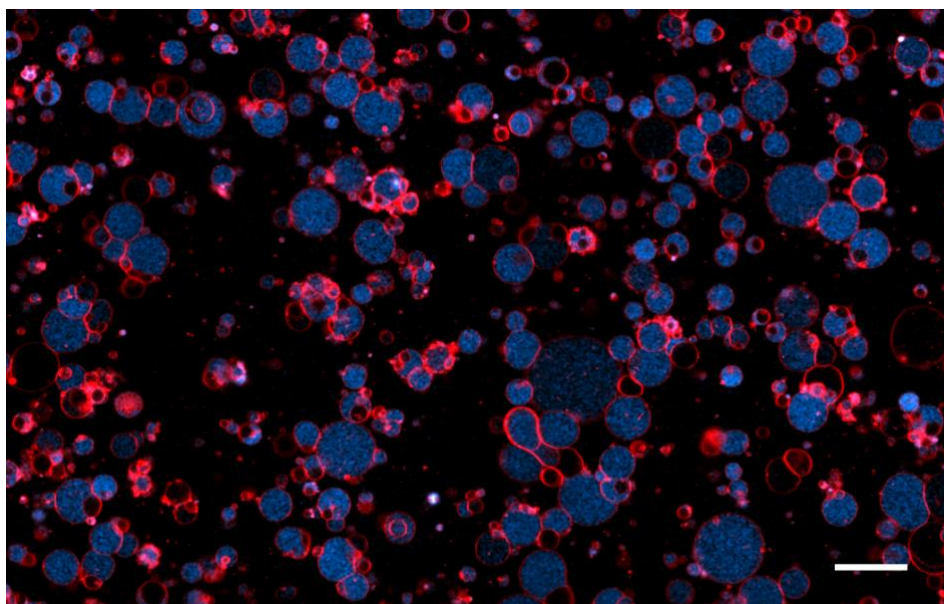


**Figure S7:** Negative control for expression of BtubA/B in liposomes. Instead of bacterial tubulin, the yeast protein Vps2 was expressed in presence of 100 nM labelled tubulin. Image acquired after 4 h incubation at 37 °C. Scale bar: 20  $\mu\text{m}$ .



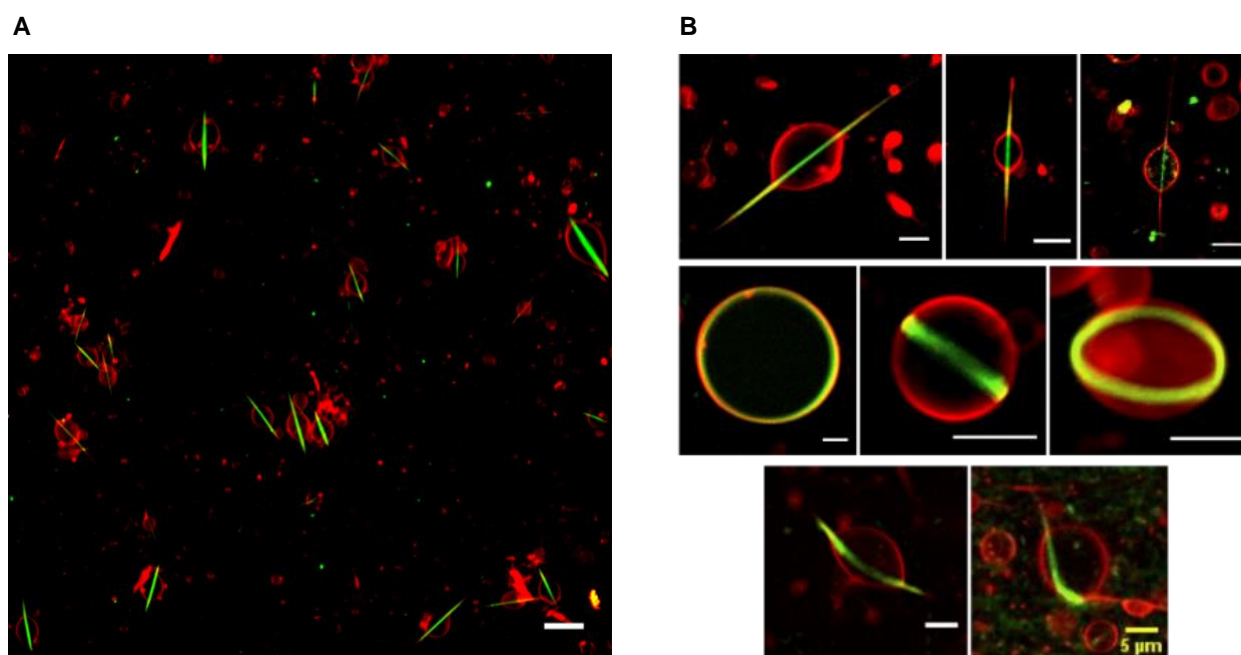


**Figure S8:** Formation of eukaryotic microtubules inside liposomes containing PURE system. (A) Confocal microscopy image of liposome populations. Purified tubulin was encapsulated at a concentration of 30 to 50  $\mu\text{M}$  (including a small fraction of tubulin labelled with HiLyte 488) in liposomes following the protocol used for the expression and reconstitution of bMTs. (B) Straight filament bundle forming  $\phi$  shaped liposomes (top row). Ring shaped bundles inside spherical liposomes (middle row). Intermediate morphology with partly bend filaments (bottom row). Images are Z-projections created by ImageJ from Z-stacks.

## **SUPPLEMENTARY MOVIES**

**Movie 1** TIRF imaging of purified bMTs doped with Atto488-labelled BtubA/B on a planar lipid bilayer. Experimental conditions are as described in Fig. 2A.

**Movie 2** TIRF imaging of purified bMTs doped with Atto488- and Atto565-labelled BtubA/B on a planar lipid bilayer. Experimental conditions are as described in Fig. 2B-D.

**Movie 3** TIRF imaging of purified bMTs doped with Atto488- and Atto565-labelled BtubA/B on a planar lipid bilayer exposed to intense illumination. Experimental conditions are as described in Fig. 2E.

**Movie 4** TIRF imaging of cell-free expressed bMTs doped with Atto488-labelled BtubA/B on a planar lipid bilayer. Experimental conditions are as described in Fig. 3.

## SUPPLEMENTARY REFERENCES

- [1] Akendengue, L., Trepout, S., Grana, M., Voegelé, A., Janke, C., Raynal, B., Chenal, A., Marco, S., and Wehenkel, A. M. (2017) Bacterial kinesin light chain (Bklc) links the Btub cytoskeleton to membranes. *Sci. Rep.* 7, 45668.
- [2] Deng, X., et al. (2017) Four-stranded mini microtubules formed by prosthecobacter BtubAB show dynamic instability. *Proc. Natl. Acad. Sci. U. S. A.* 114, E5950-58.
- [3] Blanken, D., van Nies, P., and Danelon, C. (2019) Quantitative imaging of gene-expressing liposomes reveals rare favorable phenotypes. *Phys. Biol.* 16, 45002.
- [4] Hotani, H., and Miyamoto, H. (1990) Dynamic features of microtubules as visualized by dark-field microscopy. *Adv. Biophys.* 26, 135-156.
- [5] Kuchnir Fygenson, D., Elbaum, M., Shraiman, B., and Libchaber, A. (1997) Microtubules and vesicles under controlled tension. *Phys. Rev. E* 55, 850-859.
- [6] Kuchnir Fygenson, D., Marko, J. F., and Libchaber, A. (1997) Mechanics of microtubule-based membrane extension. *Phys. Rev. Lett.* 79, 4497-4500.
- [7] Emsellem, V., Cardoso, O., and Tabeling, P. (1998) Vesicle deformation by microtubules: A phase diagram. *Phys. Rev. E* 58, 4807-4810.
- [8] Zuker, M. (2003) Mfold web server for nucleic acid folding and hybridization prediction. *Nucleic Acids Res.* 31, 3406-3415.